Int J Adv Manuf Technol (2017) 89:219–225
DOI 10.1007/s00170-016-9063-9

ORIGINAL ARTICLE

Influence of cutting parameters on the ductile-brittle transition of single-crystal calcium fluoride during ultra-precision cutting

Xiao Chen[1] · **Jianfeng Xu**[1] · **Haisheng Fang**[2] · **Ruiji Tian**[1,3]

Received: 6 February 2016 / Accepted: 15 June 2016 / Published online: 28 June 2016

Abstract The cutting mode transition from ductile to brittle is related to the depth of cut for the machining of brittle materials. The critical depth of cut for ductile to brittle transition (DBT) during single-point diamond turning of single-crystal calcium fluoride was examined, and the effect of cutting direction, cutting speed, and tool rake angles were investigated. Results show that the cutting speed had a slight effect on the critical depth of cut for DBT, while negative rake angle tools yielded large critical depth of cut for DBT. The influence of cutting direction (crystallographic orientation) on the critical depth of cut for DBT was associated to fracture toughness (K_C) of the materials. Higher K_C values induced larger critical depth for DBT. Furthermore, periodic variations of K_C values as a function of the crystallographic orientation correlated well with changes in critical depth ranging between 100 and 600 nm. This resulted in the successive emergence of brittle and ductile cutting regions when a nominal depth of cut of 0.5 μm was used, while it led to the formation of a smooth and homogenous surface with R_a of 2.838 nm at a nominal depth of cut of 0.1 μm.

✉ Jianfeng Xu
jfxu@hust.edu.cn

[1] State Key Laboratory of Digital Manufacturing Equipment and Technology, School of Mechanical Science and Engineering, Huazhong University of Science and Technology, Wuhan 430074, China

[2] School of Energy and Power Enginerring, Huazhong University of Science and Technology, Wuhan 430074, China

[3] Research Institute of Huazhong University of Science and Technology in Shenzhen, Shenzhen 518057, China

Keywords Ultra-precision cutting · Critical depth of cut · Single-crystal calcium fluoride · Fracture toughness

1 Introduction

Single-crystal calcium fluoride (CaF_2) exhibits extremely high transmissivity, excellent chromatic aberration properties, and high refractive index ranging from the ultraviolet to the infrared spectra (125 nm to 12 μm) [1]. Due to these outstanding characteristics, CaF_2 is of increasingly widespread importance in many indispensable optical components, such as semiconductor photolithography system lenses, infrared imaging system, and optical microresonators [1–5]. However, its low fracture toughness, low hardness, and high thermal expansion coefficient generates difficulties in machining CaF_2, hence hindering its applications for high-quality optical devices [1, 6, 7]. Typical CaF_2 optical components are finished by lapping and subsequent mechanical polishing [8]. These methods, however, are time-consuming and cannot be fully automated for the production of complex shapes, such as aspherical lenses and diffraction gratings [9, 10]. Single-point diamond turning (SPDT) offers opportunity to efficiently process brittle materials (e.g., silicon, germanium, silicon carbide, KDP, and BK7 glass) into complex shapes, great precision as well as low surface roughness due to the ductile regime cutting mode [11–18].

SPDT has received much attention over the past few years. Liu et al. [11] studied the relation between the critical undeformed chip thickness and the tool cutting edge radius for the brittle-ductile transition of silicon wafers chip formation. Results indicated that the ductile cutting of silicon can be achieved at specific values of the undeformed chip thickness, depending on the tool cutting edge radius. Peng et al. [12] analyzed the undeformed chip zone and its relation to the

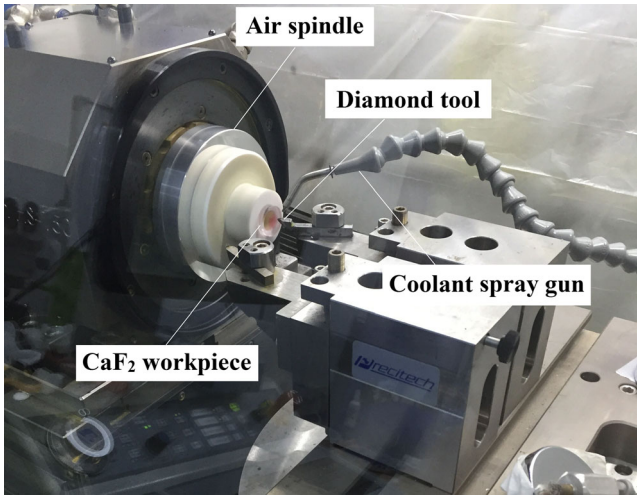

Fig. 1 Photograph of the main section of the experimental setup

critical brittle/ductile transition depth of cut by single-point diamond fly-grooving of monocrystalline silicon. A mechanics-based model was also proposed to describe the material stress condition under the diamond tool. Wang et al. [13] used a strain gradient theoretical calculation to explore the brittle-ductile transition mechanism and verified by SPDT of single-crystal silicon. Pawase et al. [14] analyzed machining mechanism in SPDT of germanium lenses, and Wang et al. [15] studied the brittle-ductile transition phenomenon in SPDT of monocrystalline germanium implanted with copper ions. Goel et al. [16] performed diamond turning of single-crystal 6H–SiC and obtained a surface finish of $R_a = 9.2$ nm. They also observed very high cutting resistance as indicated by the significant wear on the cutting tool after 1 km of cutting length. Wang et al. [17] used SPDT method for machining KDP crystals and reported high accuracy (PV value of 0.498λ) and a surface finish of $R_a = 5.3$ nm. In this work, the microwaviness of the surface and the subsurface damages were both significantly reduced by using a water dissolution procedure. Fang et al. [18] successfully achieved nanoscale surfaces by the SPDT of BK7 glass in ductile mode. This research revealed the critical role by the effective negative rake angle compared to a nominal rake angle, while tool wear was severe during cutting.

In previous studies, Yan, Azami, Kakinuma, and their co-workers [6, 7, 9, 10] showed that the SPDT of single-crystal CaF_2 induced a non-uniform surface quality due to the crystallographic anisotropy of the material. They suggested that such non-uniformity might be attributed to slip plastic deformation and cleavage fracture with continuous changes in cutting direction. Achieving ductile cutting mode is of paramount importance for excellent and uniform surface quality of CaF_2 using SPDT method. For brittle materials, the cutting mode transition from ductile to brittle is related to the depth of cut. The critical depth of cut for ductile-brittle transition (DBT) is influenced by different parameters, such as cutting direction (anisotropy of single crystal), cutting speed (varying from the center to the margin of workpieces during end face turning), and tool geometry (related to cutting force). Very limited work focused on the latter two factors during the SPDT of single-crystal CaF_2. A previous study [9] has reported the effect of cutting direction on the critical depth of cut for DBT; the analysis was, however, based on the abstract viewpoint of slip system and cleavage.

The present work consists in examining the influence of cutting directions, cutting speeds, and tool rake angles on the critical depth of cut for DBT during the SPDT of single-crystal CaF_2 using a plunge-cut method. The critical depth of cut for DBT changes with crystallographic orientation is explained by a visualized viewpoint. Moreover, the formation mechanism of the non-uniform surface after end face turning is also investigated and discussed.

2 Experimental procedures

2.1 Determination of critical depth of cut

The critical depth of cut for DBT was measured based on a plunge-cut method using a three-axis ultra-

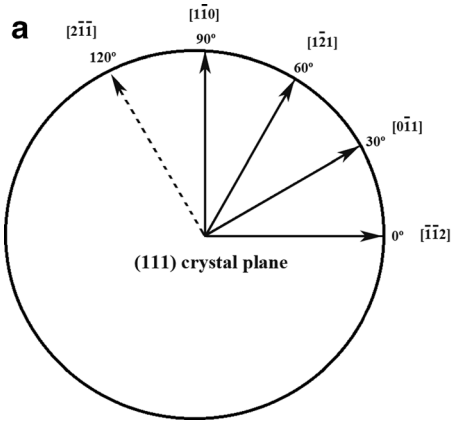

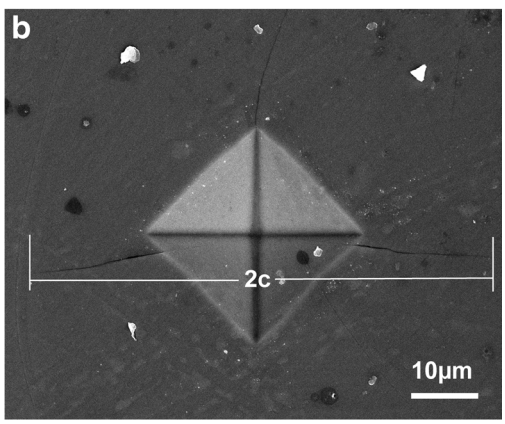

Fig. 2 Schematic of directions/orientations (**a**); SEM image of the indentation and the radial cracks caused by microhardness tester (**b**)

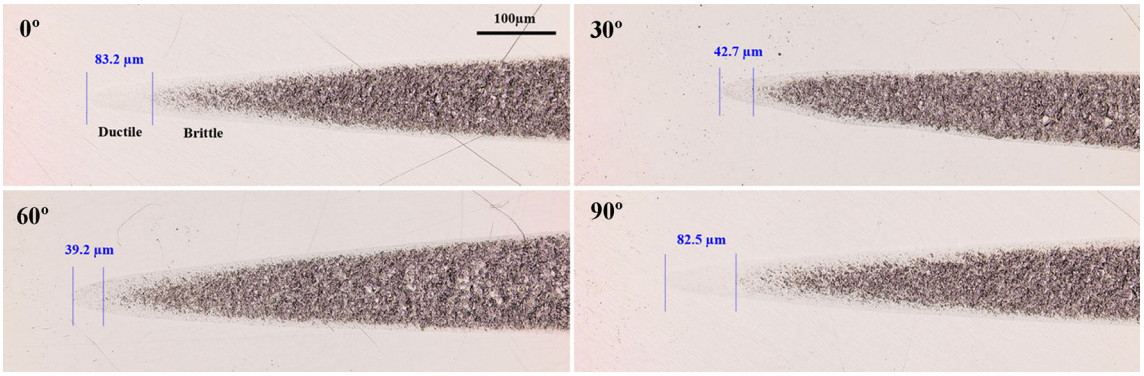

Fig. 3 The morphology of the machined microgrooves

precision machine tool (Precitech Nanoform X, USA). The main section of the setup is depicted in Fig. 1. Pre-polished, 20-mm diameter, and 5-mm thickness single-crystal CaF_2 specimens with (111) plane orientation were served as workpieces, which were vacuum-chucked to the machine spindle. Round edge natural diamond tools (Contour Fine Tooling Ltd, UK) with 5-mm nose radius were transversely fed at a constant cutting speed along the Y direction, while the depth of cut was continuously varied along the X direction from 0 to 2 μm. This technique allows the formation of a microgroove with varying depth. Triplicates of each plunge-cut test were performed to ensure credible measured data. The morphology of the microgrooves was observed using a laser scanning confocal microscope (Keyence VK-X200K, Japan), and the depth of cut was measured by nano-indentation using a scanning map mode with 2 μN contact force (Hysitron TI750, USA). The surface roughness was analyzed by atomic force microscope (AFM, SPM9700, Shimadu, Japan). A piezoelectric dynamometer (Kistler 9119AA2, Switzerland) was mounted on the diamond tool to measure microcutting forces. A coolant was employed during machining tests.

2.2 Evaluation of fracture toughness

The fracture toughness (K_C) of different crystallographic orientations of CaF_2 (Fig. 2a) was evaluated from the radial crack length caused by the microhardness tester (Qness Q10A, Austria), as depicted in Fig. 2b. The load force and the holding time were 0.98 N and 10 s, respectively. The K_C values were determined as follows [19]:

$$K_C = (0.016 \pm 0.002)\left(\frac{E}{H}\right)^{1/2}\frac{P}{C^{3/2}} \quad (1)$$

In Eq. (1), E is the Young's modulus, H represents the hardness and can be estimated from the indentation diagonal D, P corresponds to the load force, and c is the half-crack size (i.e., $2c$ is the tip to tip distance). The Young's modulus, E, and fracture toughness, K_C, of different crystallographic orientations of CaF_2 were evaluated using the average of five nano-indentation measurements along each direction. The crack sizes were analyzed using a scanning electron microscope (SEM, FEI Quanta 200, USA).

3 Results and discussion

3.1 Influence of the crystallographic orientation on the critical depth of cut

Figure 2a illustrates the crystal orientations $[\bar{1}\bar{1}2]$, $[0\bar{1}1]$, $[1\bar{2}1]$, and $[1\bar{1}0]$, labeled as 0°, 30°, 60°, and 90°, respectively. In each case (i.e., direction/orientation), the microgroove was conducted at a cutting speed of 3000 mm/min and a tool rake angle of −25°. The morphology of the as-processed

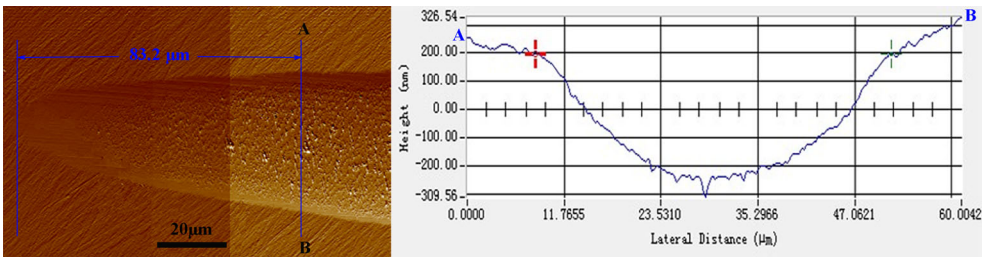

Fig. 4 The critical depth of cut for the microgroove along the 0° direction measured by nano-indentation tester

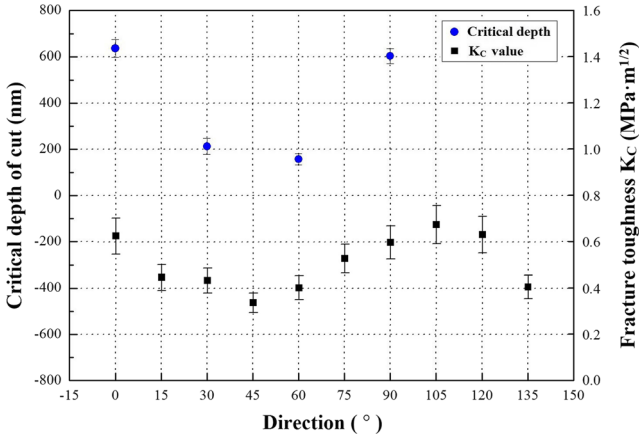

Fig. 5 The critical depth of cut and the fracture toughness versus directions

specimens is shown in Fig. 3. It can be observed that the ductile processing areas of the microgrooves along the 0° and 90° directions are larger than those along the 30° and 60°. The critical depth of cut for the microgroove in the 90° is 603.3 nm, as measured by nano-indentation, and the corresponding 3D profile exhibits a high accuracy due to the point-contact scanning of the tip (Fig. 4). The critical depths of cut in other three directions are given in Fig. 5. Noteworthy, the critical transition depths along the 0° and 90° are in the same range (i.e., about 600 nm), while they are below 200 nm both in the 30° and in the 60° directions.

Moreover, Fig. 5 shows the evolution of the fracture toughness of the CaF_2 specimen as a function of the crystal orientations. In can be seen that the fracture toughness reaches a maximum in the 105° direction ($K_C = 0.675$ MPa $m^{1/2}$), which is similar to fracture toughness reported by Corning for the production of CaF_2 ($K_C = 0.70$ MPa $m^{1/2}$) [20]. As an important property of brittle materials, fracture toughness, K_C, defines the ability of a material containing a crack to resist fracture. Higher fracture toughness indicates that it is more difficult for a crack propagate in the materials, hence increasing its resistance to the brittle fracture. Therefore, higher K_C values will lead to the larger critical depth of cut for DBT. Such trend can actually be observed in the experimental data presented in Fig. 5. To some extent, this means that the critical depth of cut for DBT might be positively correlated to fracture toughness of the materials.

3.2 Influence of the cutting speed and tool rake angle on the critical depth of cut

The effect of both cutting speed and tool rake angle on the critical depth of cut were evaluated. First, the cutting speed was increased from 2000 to 4000 mm/min in increments of 500 mm/min, and the other parameters were kept constant as follows: The tool rake angle was set to −25°, and the cutting direction was set to the 0° direction (i.e., $[\overline{1}12]$ crystal orientation). Figure 6 shows that the critical depth of cut increases slightly with the augmentation of the cutting speed and reaches a maximum at 3500 mm/min. Nevertheless, variations in the critical depth of cut remain relatively small with changes in cutting speed under the studied conditions. On the contrary, the tool rake angle exhibits a much stronger influence on the ultra-precision cutting process of brittle materials. For instance, silicon and germanium are often machined using a rake angle diamond tool of −15°~45° rake and −45°, respectively [11, 16]. Here, different rake angle tools (i.e., 0°, −15°, −25°, and −35°) were used to produce microgrooves in 0° direction (i.e., $[\overline{1}12]$ crystal orientation) and at the cutting speed of 3000 mm/min. Figure 6 shows that in the case of −15°, −25°, and −35° rake angles, the critical depth of cut exceeds 600 nm, which is three times larger than that with a 0° rake angle. Among the three negative rake angle tools,

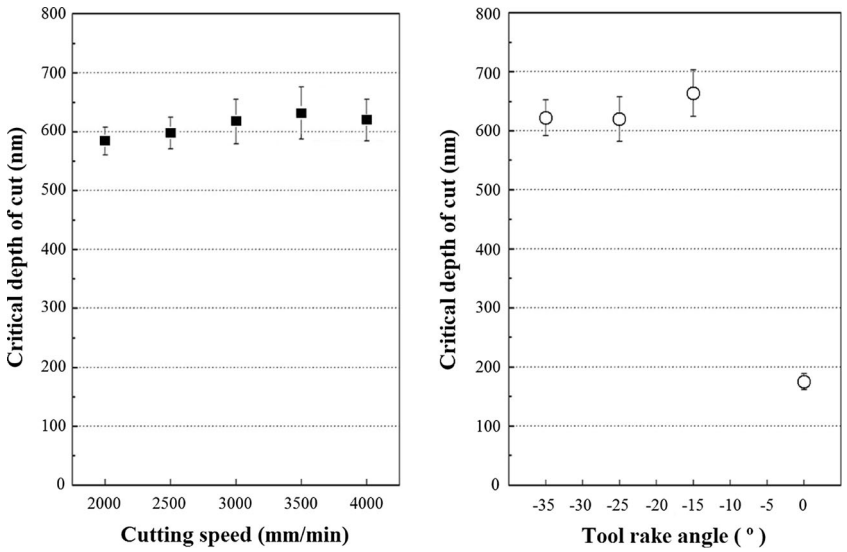

Fig. 6 The cutting speeds and the tool rake angles versus critical depths of cut

−15° rake angle is the most appropriate tool geometry for CaF_2 machining, since it leads to the largest critical depth of cut. During plunge-cut process, the cutting force was measured for different rake angle tools, as presented in Fig. 7. It is noteworthy that the larger cutting force yields the smaller critical depth of cut. This can be attributed to the fact that larger cutting forces induced an earlier transition of the cutting mode from ductile to brittle during the plunge-cut process.

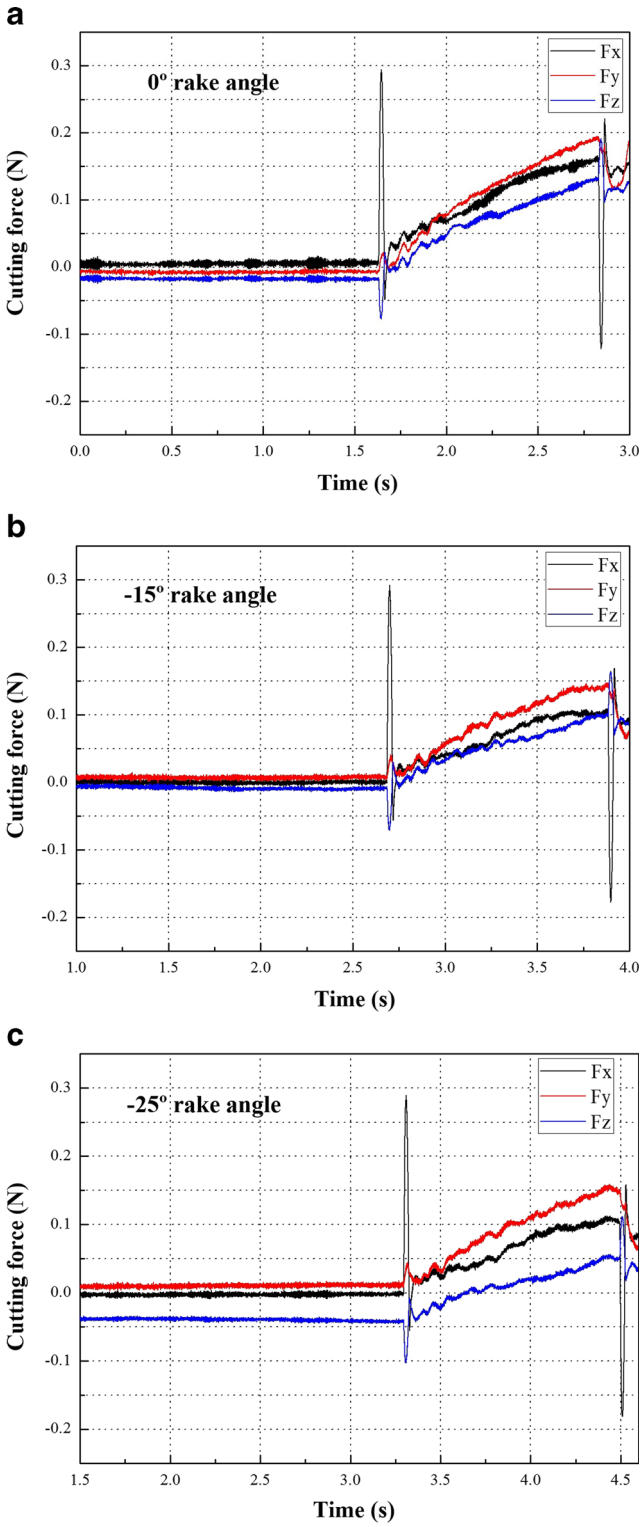

Fig. 7 The cutting force for different rake angle tools during the plunge-cut process

3.3 The surface quality machined by end face turning

CaF_2 specimens were machined using a −15° rake angle diamond tool under the following conditions: 3000 rpm spindle speed, 1 μm/r feed rate, and 0.5 and 0.1 μm nominal depths of cut. In Fig. 8a, it can be observed that two distinct regions with different brightness appeared alternately when a depth of cut of 0.5 μm was used. However, when the depth of cut is reduced to 0.1 μm, a uniform surface is obtained as illustrated in Fig. 8b. A similar phenomenon has previously reported by Yan et al. [6, 7]. The surface roughness was analyzed by AFM, and the results are presented in Fig. 9. The surface quality of the darker regions in Fig. 8a is relatively poor due to brittle cutting mode (Fig. 9a), while the brighter regions in Fig. 8a and the region in Fig. 8b exhibit a smooth surface (R_a are 2.678 and 2.838 nm, respectively) due to ductile cutting mode (Fig. 9b, c). Although the surface quality in Fig. 9b, c have similar R_a, R_q, and R_v values, the R_z and R_p values of the former are larger than those of the latter, thus revealing that better surface quality can be achieved using smaller depth of cut. Figure 10 is an SEM photograph of the chips generated under the condition of 0.1 μm nominal depth of cut. The chips are continuous ribbons, similar to those produced in the case of metal cutting, which indicates that the workpiece has been removed in a ductile mode.

4 Discussion

As described above, the distribution of brittle and ductile regions in Fig. 8a can be correlated to the critical depth of cut for DBT (Fig. 5). This reveals that cutting directions with small critical depth of cut lead to brittle cutting mode, while cutting directions with large critical depth of cut resulted in ductile cutting mode. During the cutting process, all crystal orientations are continuously scratched by the diamond tool edge. At a constant nominal depth of cut of 0.5 μm, brittle cutting mode occurs in the crystal orientation where it possesses a small critical depth of cut (such as 30° and 60°, Fig. 5). On the other hand, ductile cutting mode happens in other crystal orientation where it possesses a large critical depth of cut (such as 0° and 90°, Fig. 5). Furthermore, in the case when the nominal depth of cut (i.e., 0.1 μm) is smaller than the minimum critical depth of cut for DBT, ductile cutting mode occurs regardless of the crystal orientation, hence forming homogenous and smooth surface.

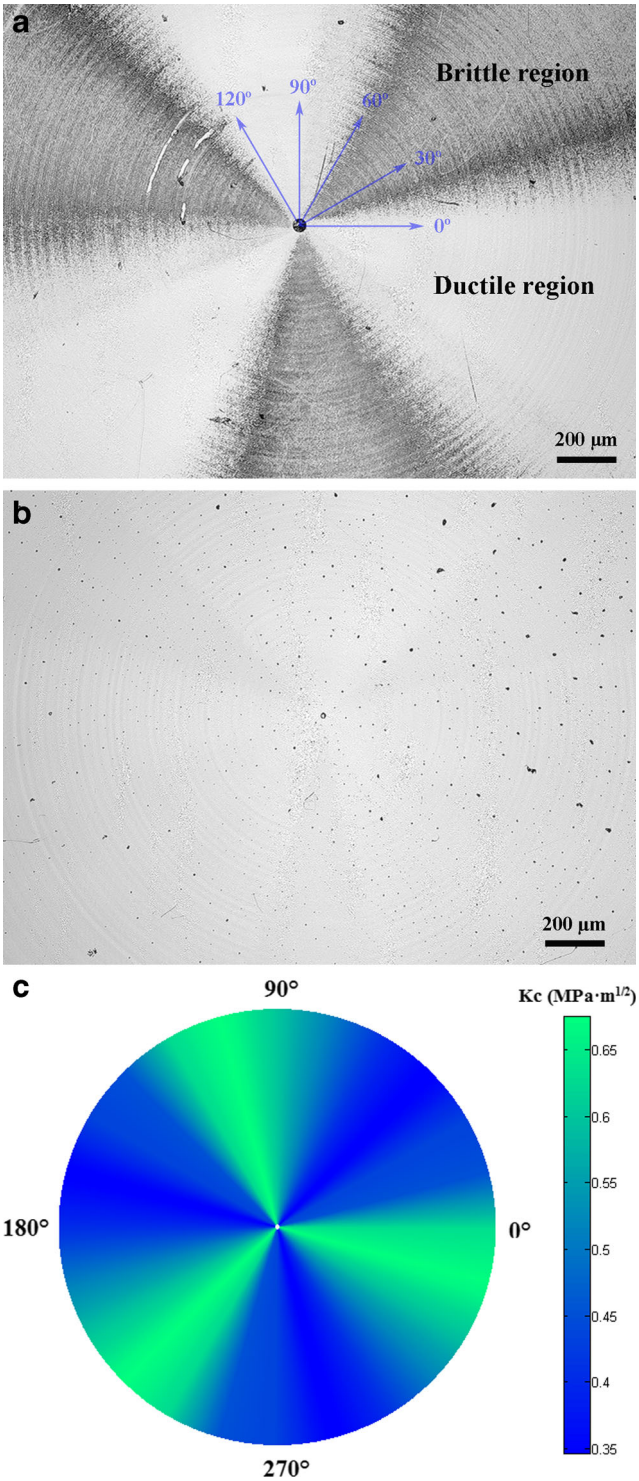

Fig. 8 The surface morphology and K_C value distribution of the CaF_2: **a** machined by a depth of cut of 0.5 μm, **b** machined by a depth of cut of 0.1 μm, and **c** distribution of K_C plotted by MATLAB

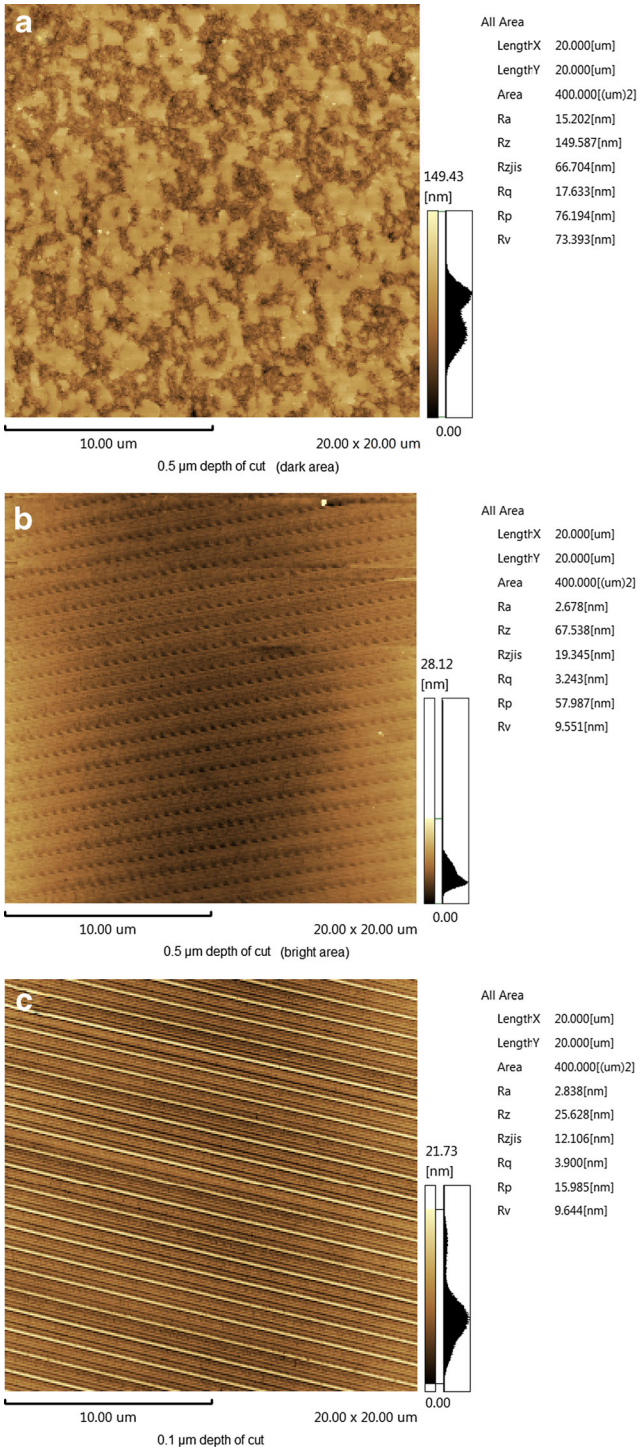

Fig. 9 The surface roughness of CaF_2 after end face turning

The critical depth of cut for DBT inherently depends on the fracture toughness, K_C, which arises from the anisotropic properties of single crystals. Noteworthy, the K_C value seems to vary periodically every 120° cycles, as shown in Fig. 5. Periodicity is an essential characteristic of crystals. Assuming that each K_C value corresponds to a different crystal orientation in a periodic cycle of 120°, the distribution of K_C values can be plotted as shown in Fig. 8c. By comparing Fig. 8a, c, it can be observed that the distribution of K_C values follows a similar trend as that of brittle and ductile regions, with three high K_C regions and three low K_C regions presenting alternately, forming a non-uniform surface.

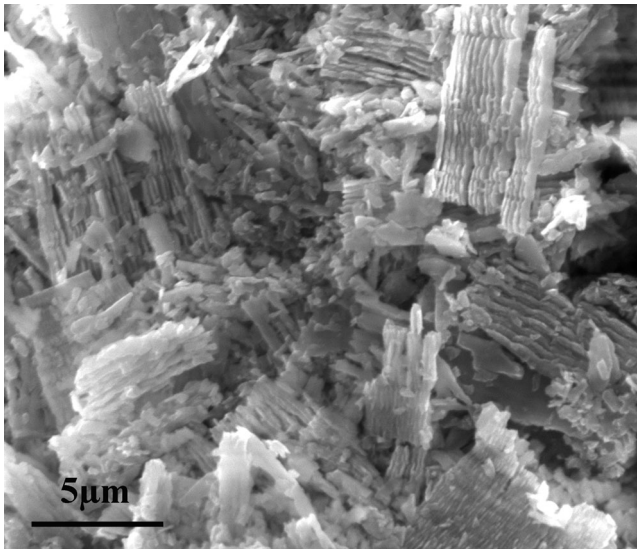

Fig. 10 SEM photograph of continuous CaF_2 chips

5 Conclusions

In summary, large critical depth of cut for DBT can be correlated to high fracture mechanical property. The critical depths of cut along the $[\bar{1}\bar{1}2]$ and $[1\bar{1}0]$ orientations were about 600 nm, which was three times larger than those along the $[0\bar{1}1]$ and $[1\bar{2}1]$ orientations. Cutting speed exhibited little influence on the critical depth of cut in the range of 2000–4000 mm/min. Diamond tool with negative rake angles showed larger critical depth of cut due to smaller cutting force during the plunge-cut process. A homogeneous smooth surface with 2.838 nm R_a was obtained at a nominal depth of cut of 0.1 μm, while a non-uniform surface with alternate brittle and ductile cutting regions was generated when larger nominal depth of cut was employed.

Acknowledgments This research is funded by the National Natural Science Foundation of China (51375195) and Science and Technology Plan Projects of Shenzhen City (JCYJ20140903171444755). The authors thank the Analytical and Testing Center of Huazhong University of Science and Technology.

References

1. Kaminskii A (2013) Laser crystals: their physics and properties. Springer
2. Lee B, Lehmann K, Taylor J, Yalin A (2014) A high-finesse broadband optical cavity using calcium fluoride prism retroreflectors. Opt Express 22:11583–11591
3. Zhang Z, Hu B, Yin Q, Yu T, Li S, Gao X, Zhang H (2015) Design of short wave infrared imaging spectrometer system based on CDP. Opt Express 23:29758–29763
4. Qi Y, Zhang T, Cheng Y, Chen X, Wei D, Cai L (2016) Lattice dynamics and thermal conductivity of calcium fluoride via first-principles investigation. J App Phys 119:095103
5. Hahn D (2014) Calcium fluoride and barium fluoride crystals in optics. Optik & Photonik 9(4):45–48
6. Yan J, Syoji K, Tamaki J (2004) Crystallographic effects in micro/nanomachining of single-crystal calcium fluoride. J Vac Sci Technol B 22:46–51
7. Yan J, Tamaki J, Syoji K (2004) Single-point diamond turning of CaF2 for nanometric surface. Int J Adv Manuf Tech 24:640–646
8. Yin G, Li S, Xie X, Zhou L (2014) Ultra-precision process of CaF2 single crystal. Proceedings of SPIE, 7th International Symposium on Advanced Optical Manufacturing and Testing Technologies (AOMATT 2014), International Society for Optics and Photonics 9281.
9. Azami S, Kudo H, Mizumoto Y, Tanabe T, Yan J, Kakinuma Y (2015) Experimental study of crystal anisotropy based on ultra-precision cylindrical turning of single-crystal calcium fluoride. Precis Eng 40:172–181
10. Kakinuma Y, Azami S, Tanabe T (2015) Evaluation of sub-surface damage caused by ultra-precision turning in fabrication of CaF2 optical micro resonator. CIRP Ann-Manuf Techn 64:117–120
11. Liu K, Li X, Rahman M, Neo K, Liu X (2007) A study of the effect of tool cutting edge radius on ductile cutting of silicon wafers. Int J Adv Manuf Tech 32:631–637
12. Peng Y, Jiang T, Ehmann K (2014) Research on single-point diamond fly-grooving of brittle materials. Int J Adv Manuf Tech 75: 1577–1586
13. Wang M, Wang W, Lu Z (2013) Critical cutting thickness in ultra-precision machining of single crystal silicon. Int J Adv Manuf Tech 65:843–851
14. Pawase P, Brahmankar P, Pawade R, Balasubramanium R (2014) Analysis of machining mechanism in diamond turning of germanium lenses. Procedia Mater Sci 5:2363–2368
15. Wang J, Fang F, Zhang X (2015) An experimental study of cutting performance on monocrystalline germanium after ion implantation. Precis Eng 39:220–223
16. Goel S, Luo X, Comley P (2013) Brittle-ductile transition during diamond turning of single crystal silicon carbide. Int J Mach Tools Manuf 65:15–21
17. Wang X, Gao H, Chen Y, Guo D (2015) A water dissolution method for removing micro-waviness caused by SPDT process on KDP crystals. Int J Adv Manuf Tech: 1–14
18. Fang F, Zhang G (2004) An experimental study of optical glass machining. Int J Adv Manuf Tech 23:155–160
19. Fang T, Lambropoulos JC (2002) Microhardness and indentation fracture of potassium dihydrogen phosphate (KDP). J Am Ceram Soc 85:174–178
20. Ladison J, Price J, Helfinstine J (2005) Hardness, elastic modulus, and fracture toughness bulk properties in Corning calcium fluoride. Proceedings of SPIE, Optical Microlithography 5754:1329–1338